An efficient Two-Layer wall model for accurate numerical simulations of aeronautical applications.

Joan Calafell⋆*, Francesc-Xavier Trias*⋆ *and Assensi Oliva*⋆†
⋆*Heat and Mass Transfer Technological Center*
Colom 11, 08222 Terrassa (Barcelona)
joancs@cttc.upc.edu · xavi@cttc.upc.edu
†oliva@cttc.upc.edu

Abstract

Two-Layer wall models have been widely studied since they allow wall modeled Large Eddy Simulations of general non-equilibrium flows. However, they are plagued by two persistent problems, the "log-layer mismatch" and the resolved Reynolds stresses inflow. Several methodologies have been proposed so far to deal with these problems separately. In this work, a time-filtering methodology is used to tackle both issues at once with a single and low-computational-cost step, easily applicable to complex three-dimensional geometries. Additionally, it is shown that the techniques intended to suppress the Reynolds stresses inflow proposed so far, were not sufficient to completely mitigate their detrimental effects.

Introduction

Wall-bounded flows at high Reynolds number are of capital importance in the aeronautical industry. A deeper understanding of their physics would lead to more optimized aerodynamic designs. Nonetheless, the routine use of accurate numerical methodologies such as Large Eddy Simulation (LES) for these particular flow conditions, is still extremely costly due to their heavy computational cost. Wall-Modeled LES (WMLES) is intended to circumvent the massive costs of accurately resolving the boundary layer while benefiting from the temporal and spatial resolution of an LES computation.

Several works attempting to estimate the advantages of using WMLES instead of WRLES can be found in the literature. Choi and Moin[9] proposed two expressions for the Reynolds number scaling of the computational cost associated with the spatial resolution for each methodology. Later, Calafell et al.,[6] took also into account the costs associated with time integration. By combining temporal and spatial costs, the authors proposed a new set of Reynolds scaling expressions: For WRLES, the computational costs scale proportionally to $Re_{L_x}^{3.09}$, while for WMLES, the scaling law is proportional to only $Re_{L_x}^{1.33}$ which highlights the huge benefits of wall modeling, especially at high Reynolds numbers.

The present work is focused in Two-Layer wall models (TLM) based on Unsteady Reynolds Averaged Navier Stokes (URANS). This approach allows WMLES of complex unsteady non-equilibrium flows. This makes them a suitable choice for the simulation of industrial flows since non-equilibrium conditions are widespread in most practical applications.

The zonal or Two-Layer model (TLM) approach was initially proposed by Balaras *et al.*[2,3] The methodology is based on the resolution of the URANS equations or a simplified variant in a fine auxiliary mesh that is embedded in the LES domain between the solid boundary and the first off-wall node row (see Figure 1). The boundary conditions for the URANS domain are taken from the LES nodes at the LES/TLM interface, while the time integration is carried out with implicit or semi-implicit schemes to avoid restrictions due to stability considerations. This allows obtaining an accurate near-wall velocity field from which a precise wall shear stress is derived and supplied to the LES computation as the wall model output.

Nevertheless, the TLM approach is affected by two recurrent problems which are common to other wall modeling approaches. A persistent problem is the "log-layer mismatch" (LLM) which, according to Cabot and Moin[5] and Kawai and Larsson,[11] is a consequence of the presence of large numerical and subgrid errors in the near-wall nodes. When taking LES data from these nodes, these errors are introduced into the wall model, causing spurious values of the model output. On the other hand, in the TLM strategy, when the convective term is considered in the model physical

DOI: 10.13009/EUCASS2019-694

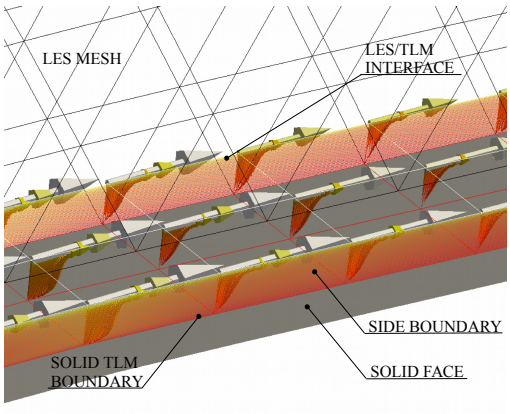

Figure 1: The two-layer strategy scheme.

formulation, a particular source of error appears due to the inflow of resolved Reynolds stresses (RRS) of the LES domain into the wall layer.[4]

Several strategies have been proposed so far to mitigate the LLM[11,21] and the RRS inflow[11,15] problems separately. Nevertheless, most of the proposed methodologies have a significant computational cost, or in some cases, a lack of generality, making the overall efficiency and generality of the wall model (WM) to drop dramatically. The strategy proposed in this work is based on applying a time-averaging filter (TAF) to the WM/LES interface. This methodology allows blocking the RRS inflow while avoiding the LLM problem at the same time, with a single, simple, and low-computational-cost technique boosting the WM efficiency compared to other existing techniques. The TAF technique was firstly introduced by Yang *et al.*[22] to stabilize the computation of an integral boundary layer wall model by making physically consistent the model input with its mathematical formulation. More recently, Yang *et al.*[21] reported good results by taking the WM input data from the first row of off-wall nodes when applying the TAF to a simple equilibrium wall function. According to the authors, the TAF breaks the unphysical temporal synchronization between the LES velocity at the first off-wall nodes and the wall shear stress, which according to the new theory developed in their work, it is the origin of the LLM.

In the present work, the TAF technique is applied to a TLM for the first time. In this context, the primary mission of the TAF is blocking the RRS inflow, being the first time that a TAF is used for this purpose. According to the results presented in sections below, this approach performs significantly better in blocking the RRS inflow compared to other methods proposed so far.[15] In fact, it is shown that the techniques published until now were not able to tackle all the undesired effects of the RRS. Therefore, taking into account the present results and the findings of Yang *et al.*, the TAF can suppress the LLM and the RRS inflow problems at once with a single step and with a fraction of the computational cost of previously proposed methods.[11,15] For more details, the reader is referred to the extensive reviews on wall modeling and two-layer wall models published by Piomelli and Balaras[17] in 2002 and Larsson *et al.*[13] in 2015.

In order to analyze in detail the performance of the TAF in suppressing the RRS inflow, a numerical experiment based on a pipe flow test at $Re_\tau \approx 500$ will be carried out. A methodology to determine the appropriate temporal filter width, T, based on the velocity power spectrum analysis, will be proposed before performing the numerical test. Afterward, the WM performance will be assessed under regular operating conditions. This will be carried out by performing WMLES of an equilibrium pipe flow at $Re_\tau \approx 3000$. All the obtained numerical results will be compared with DNS data from different authors depending on the test.[1,8]

Mathematical and numerical method

In this Section, details of the mathematical and numerical methodologies of both, the LES and the WM domains are given.

LES domain mathematical and numerical strategy

The LES domain is governed by the spatially filtered Navier-Stokes equations:

$$\nabla \cdot \overline{u} = 0, \tag{1}$$

DOI: 10.13009/EUCASS2019-694

$$\frac{\partial \overline{u}}{\partial t} + (\overline{u} \cdot \nabla)\,\overline{u} + \nabla \overline{p} - \nu \nabla^2 \overline{u} = \nabla \cdot \left(\overline{u}\,\overline{u}^T - \overline{uu^T} \right) \approx -\nabla \cdot \tau(\overline{u}), \tag{2}$$

where $\overline{(\cdot)}$ is the spatial filtering operator, u the velocity field, p the kinematic pressure and $\tau(\overline{u})$ the subgrid stress tensor which is modelled according the Boussinesq hypothesis for incompressible flows:

$$\tau\,(\overline{u}) = -2\nu_{sgs} S\,(\overline{u}), \tag{3}$$

where $S\,(\overline{u})$ is the rate-of-strain tensor $\left(S\,(\overline{u}) = \frac{1}{2}\left(\nabla \overline{u} + \nabla \overline{u}^T \right) \right)$ and ν_{sgs} is the subgrid viscosity.

To close the formulation, an expression for ν_{sgs} must be given. In the present work, the Germano[10] dynamic approach of the Smagorinsky model with the modifications of Lilly[14] will be used. This LES closure has been selected to allow comparison with other works published in the literature since most of them use this LES approach.

To obtain a numerical solution, the equations presented above are solved through the finite volume method in a collocated unstructured grid. The spatial discretization is carried out through a second-order symmetry-preserving and a central difference scheme for the convective and diffusive terms, respectively. Such schemes preserve the symmetry properties of the continuous differential operators which ensures the stability and the conservation of the kinetic-energy balance even at high Reynolds numbers and coarse grids.[20] Regarding the temporal discretization, a second-order one-step explicit scheme for the convective and diffusive terms[19] is applied, while for the pressure, an implicit first-order scheme is used. Finally, a projection method is applied to solve the pressure-velocity coupling.

Two-Layer model mathematical and numerical strategy

As commented in the introduction section, the present TLM strategy is based on the implicit resolution of the full three-dimensional URANS equations (4) in a fine embedded mesh which stretches from the wall up to the first off-wall row of nodes (see Figure 1).

$$\frac{\partial U}{\partial t} + (U \cdot \nabla)\,U = \nabla \cdot [2(\nu + \nu_{Twm}) S\,(U)] - \nabla P, \tag{4}$$

where the capital letters stand for time-averaged magnitudes, and ν_{Twm}, is the RANS turbulent viscosity for the WM.

The equations are also solved through the finite volume methodology. The numerical schemes are the same as those used for the LES domain. On the other hand, the velocity-pressure coupling has been solved through a projection method while the temporal integration is performed through Euler's first-order implicit scheme.[16] The present implicit projection method includes a pressure-correction step to allow second-order accuracy in the pressure field resolution.[7] The implicit approach is used to avoid numerical stability problems derived from the use of large time-step in the WM computation imposed by the LES domain CFL.

The turbulence model used in the present implementation to evaluate ν_{Twm}, is a mixing-length model which has been applied in most previous TLM implementations,[3,11,15] obtaining satisfactory results even in non-equilibrium conditions.

$$\nu_{Twm} = (\kappa y^+)^2\,|S|\,[1 - exp\,(-y^+/A^+)]^2\,, \tag{5}$$

where $\kappa = 0.41$ is the von Kármán constant, y^+ is the wall distance in wall units, $|S|$ is the magnitude of the rate-of-strain tensor and $A^+ = 26$ is a wall-damping function constant.

As a boundary condition for the WM RANS computation, LES data is taken at the WM/LES interface and applied to the numerical resolution of the equations within the WM layer. Once an accurate near-wall velocity field has been obtained, it is used to compute a precise wall shear stress which is fed back to the LES domain through the solid boundary faces.

Before proceeding with the wall model description, some key concepts related to different possible dissipation sources in a given numerical simulation will be defined. Following Pope's nomenclature, we define as apparent diffusivity the inherent diffusive effects of the time-resolved flow structures on the mean flow.[18] In any time-resolving methodology for the Navier-Stokes physical model, i.e., DNS or LES, these diffusive effects are not explicitly introduced, but they are an indirect consequence of the time-resolved fluctuations. By contrast, when turbulent scales are not fully resolved, their diffusive effects must be introduced externally to keep a physically realistic model. This is carried out through the introduction of an additional viscosity to the diffusive term, which is provided by a RANS or an LES model depending on the simulation nature. This source of diffusivity is named as modeled diffusivity.

The RANS approach is intended to exclusively resolve the mean flow, while the effects of the whole fluctuating component (Reynolds stresses) are modeled through the turbulent viscosity, ν_T. Therefore, if additional time-resolved

DOI: 10.13009/EUCASS2019-694

fluctuations are introduced in a RANS domain through the boundary by the advective term, their apparent diffusive effects will be added to the RANS modeled ones, which already account for the whole fluctuating field. This is the origin of the RRS inflow problem pointed out Cabot *et al.*[4] Nonetheless, to the authors best knowledge, all the methodologies proposed until now to deal with this issue are only focused on the apparent diffusivity effects of the RRS.[5,11,15] In the following Section, we will show that this approach is insufficient and that other undesirable consequences of the RRS must be taken into account.

In our implementation, a time-averaging filter is proposed to avoid the unwanted effects of the RRS inflow. The TAF is applied to the LES variables before being used as boundary conditions for the WM. The purpose of the method is to suppress the small-scale resolved turbulent fluctuations while keeping the large-scale motion effects. Additionally, according to Yang et al.,[21] the TAF also tackles the LLM problem, allowing to solve the two recurrent problems which affect the Two-Layer models with a single and low-computation-cost step.

The filtering process is carried out through a numerical exponential running average method,[15,22] which is defined as follows for a given variable ϕ:

$$\overline{\phi}^n = (1-\epsilon)\overline{\phi}^{n-1} + \epsilon\phi^n \quad ; \quad \epsilon = \frac{\Delta t/T}{1+\Delta t/T}, \tag{6}$$

where $\overline{(\cdot)}$ is the time filtering operator, Δt is the time-step at iteration n, and T is the filter characteristic time-scale or filter length. The filtering operation in equation 6 is the numerical solution to the ordinary differential equation $\partial\overline{\phi}/\partial t = (\phi - \overline{\phi})/T$, whose exact solution is $\overline{\phi}(t) = \int_0^t \phi(\xi)\frac{exp[(\xi-t)/T]}{T}d\xi$.[15] Therefore, $\overline{\phi}$ may be considered as the local time-average of ϕ with an exponential decaying memory, being the decaying speed dependent on the value of T.

In the following sections, a methodology based on the power spectrum of the velocity components is proposed to determine the optimal filter's length, T. Time and its related magnitudes will be measured in non-dimensional time units, TU, which for the pipe flow tests presented below are defined as $1TU = R/\overline{U}$, where R is the pipe radius whereas $\overline{U}$ is the flow bulk velocity.

TAF efficiency test

In order to evaluate the TAF efficiency in suppressing the unwanted RRS effects, an assessment test has been performed. The strategy is based on a wall-resolved pipe flow at $Re_\tau = u_\tau R/\nu \approx 500$, where u_τ is the skin friction velocity. The TLM is embedded between the wall and a height of $y^+ \approx 150$, well into the logarithmic law region, which is a plausible operation position of the WM at high Reynolds number. The wall model is fed with LES data taken at the WM/LES interface while the model output, τ_w, is not used to fed back the LES domain (See figure 2).

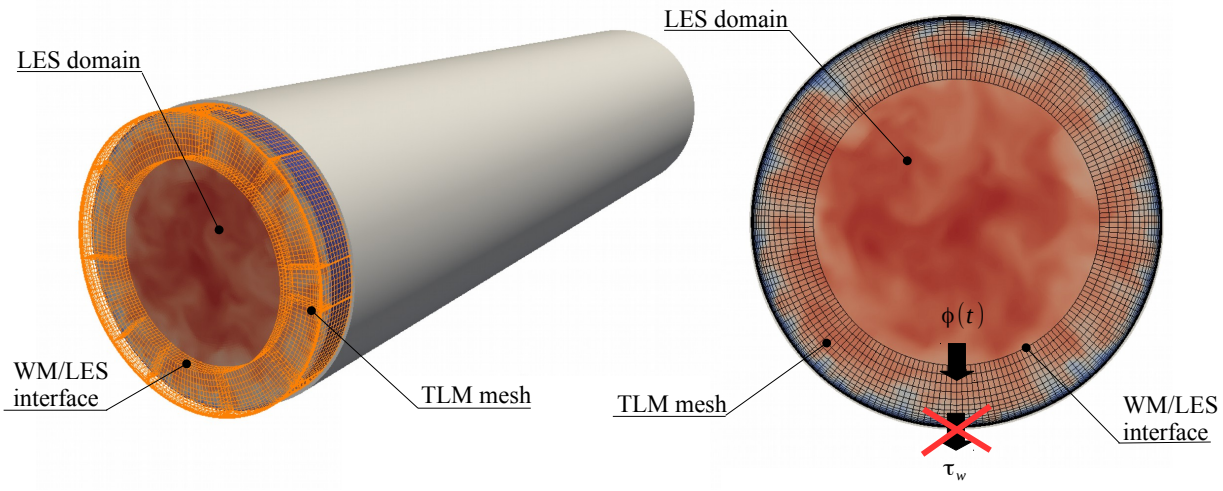

Figure 2: Time-averaging filter efficiency test scheme.

The main purpose of the test is analyzing the ability of the model in reproducing the flow physics within the wall layer, i.e., the mean velocity profile and the wall shear stress, τ_w. These parameters will be used to assess the filter efficiency in blocking the RRS inflow by comparing numerical results with reference data. Additionally, the apparent and the modeled diffusivity levels within the wall layer will be analyzed to determine the effects of the RRS inflow on

DOI: 10.13009/EUCASS2019-694

the numerical predictions as well as the influence of the filter on them. As a measure of the apparent diffusivity, the expression proposed by Park and Moin[15] to quantify these effects with a viscosity-like magnitude, ν_{ap}, will be used:

$$\nu_{ap} = -\frac{R(\mathbf{U})S^d(\mathbf{U})}{2S^d(\mathbf{U})S^d(\mathbf{U})}, \tag{7}$$

where $S^d(\mathbf{U})$, is the deviatoric part of the rate-of-strain tensor, and $R(\mathbf{U})$, is the resolved part of the Reynolds stress tensor. Although the evaluation of $R(\mathbf{U})$ requires the spatial average in an homogeneous direction,[13,15] Equation 7 is applicable for the present test.

On the other hand, DNS data of Chin *et al.*[8] is used as a reference for the mean velocity profiles while the capability of the model to determine an accurate wall shear stress is verified by computing the Re_τ and comparing it with the reference value of $Re_\tau \approx 500$.

Computational setup

The WRLES computations are performed in a domain of length of $8R$. This domain size exceeds the minimum length of $2\pi R$ required to obtain accurate one-point first and second-order statistics[8] for a $Re_\tau \approx 500$. The grid has been generated by extruding a plane mesh along the streamwise direction. The two-dimensional (2D) mesh is a structured grid with square-shaped control volumes (CV) in the region between $r = 0.5R$ and $r = R$, while between the pipe center and $r = 0.5R$, an all-triangles unstructured pattern is used. The use of different meshing patterns depending on the region is intended to avoid the wedge-shaped cells at the pipe axis which cause a significant unphysical time-step reduction. The total number of grid points of the LES mesh is 6×10^6 distributed as follows: in the outer region ($r \in [0.5R, 1.0R]$), $N_z = 256$, $N_\theta = 192$ and $N_r = 60$, being z the streamwise, θ the azimuthal and r the radial directions, while in the inner region ($r \in [0, 0.5R]$), the unstructured mesh is also extruded in 256 planes. The grid spacings in wall units are $\Delta z^+ \approx 15$, $\Delta r\theta^+ \approx 16.5$ at $r = R$ and $\Delta r^+ \approx 1.2$ at the wall, being $\Delta y_1^+ \approx 0.6$. Regarding the WM configuration, the WM/LES interface is placed at $y^+ \approx 150$, matching the top boundary nodes with their LES counterparts to avoid the necessity of numerical interpolation. The WM mesh is extruded in 20 layers and refined towards the wall, being the first off-wall node well into the viscous sublayer at a distance of $y_1^+ = 0.54$. This generates a grid which features 9.8×10^5 inner nodes. As a subgrid strategy for the LES domain, as commented in the introduction section, the dynamic Smagorinsky model has been used. Periodic boundary conditions are prescribed in the streamwise direction while no-slip and Neumann conditions are applied to the wall for velocity and pressure, respectively. The flow is enforced by keeping a constant mass flow rate consistent with the Reynolds number of $Re = 2R\overline{U}/\nu$. According to Blasius correlation, a $Re_\tau \approx 500$ pipe flow corresponds to a $Re = 1.7 \times 10^4$ based on the bulk velocity.

The temporal integration span and the averaging periods for the statistics collection are as follows: the WRLES computation has been advanced 100 flow-through cycles to reach the statistically stationary regime. Then, the WM has been coupled to the LES solution, and an additional transient period of $100\,TU$ has been run. Finally, the WM averaged variables have been collected along $100\,TU$, which corresponds to ten flow through periods, i.e., 10 times the largest flow structures appearing in the velocity energy spectrum.

Time averaging filter length setup

Finally, the temporal filter averaging period, T, has to be determined. Hereafter, a methodology is proposed to determine the optimal filter width, which is applicable for any flow condition. The strategy is based on computing the power spectrum of the most representative velocity component at the WM/LES interface. This will provide insight into the flow structures present in that region and their characteristic time-scales. Since the incoming RRS are engendered by these near-wall turbulent structures, this approach will provide valuable data about the temporal behavior of RRS that are being introduced into the wall layer, and therefore, which filter sizes have to be applied to block their spurious effects.

In Figure 3, the power spectrum of the signal of the streamwise velocity component taken at the WM/LES interface ($y^+ \approx 150$) is shown. Several characteristic frequencies in the spectrum have been selected to perform the analysis. Specifically, the frequency corresponding to the largest flow scale, a frequency within the energy-containing range, the inertial/energy-containing range limit and the inertial/dissipation range bound have been chosen. In Table 1, the selected frequencies and their corresponding temporal filter widths, T, are summarized.

TAF efficiency test results

In Table 2, results concerning the Re_τ computed by the WM for cases from 1 to 5 are shown. On the other hand, in Figure 4, the mean velocity profiles for the same configurations are displayed and compared with the DNS data of Chin

DOI: 10.13009/EUCASS2019-694

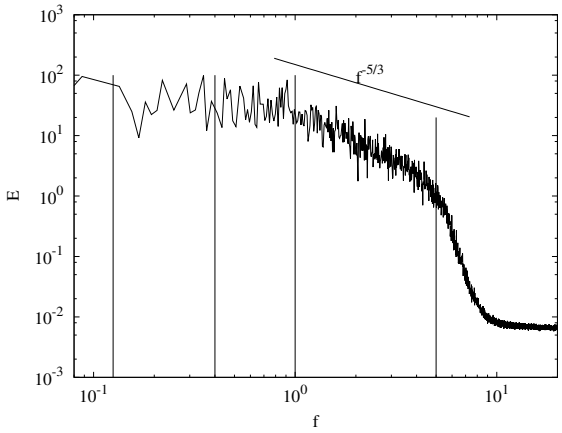

Figure 3: Power spectrum of the streamwise velocity component at $y^+ \approx 150$ of a Pipe flow at $Re_\tau \approx 500$.

Table 1: Summary of the different filter configurations for the TAF efficiency test, with their respective filter lengths, T, and their position in the energy spectrum.

Test number (n)	$f_n = 1/T_n$	Filter length T_n	Energy spectrum range
1	no filter	no filter	N/A
2	5.0	0.2	inertial/dissipation range limit
3	1.0	1.0	inertial/energy-containing range limit
4	0.4	2.5	within the energy-containing range
5	0.125	8.0	flow-through period, largest flow scales

et al.[8]

Table 2: TAF efficiency test results performed with a channel flow at $Re_\tau \approx 500$. The WM computed Re_τ and its relative error with respect to the target value ($Re_\tau \approx 500$) is shown.

Test (n)	Filter length T_n	Computed Re_τ	rel. err. [%]
1	no filter	528.70	5.74
2	0.2	515.66	3.13
3	1.0	506.81	1.36
4	2.5	502.06	0.41
5	8.0	502.18	0.43

Both, the mean velocity profiles and the wall shear stress results are in line with the findings of Cabot and Moin.[5] The incoming RRS cause a diffusivity excess in the wall domain since the RANS model already provides the diffusivity associated with any fluctuating, i.e., time-resolved, component. This effect is evidenced in test 1, in which no measure to block the RRS inflow is applied. Both, the mean velocity profile and the wall shear stress are clearly overpredicted. As the time-resolved component of LES is prevented from entering the RANS domain by increasing the temporal filter length, the shear stress and the mean velocity profile converge progressively to their respective references. According to the values displayed in Table 2 and Figure 4, satisfactory results are obtained when the cut-off filter length is set approximately at frequencies lower than the inertial subrange ones. For higher frequencies (at the beginning of the dissipation range) the averaging period is not enough to sufficiently block the RRS inflow, although significant improvement is observed compared to the non-filtered solution.

To analyze in deeper detail the effects of RRS inflow on the wall layer physics prediction, the levels of apparent and modeled diffusivities within the wall layer will be analyzed for different temporal filter sizes. The two different diffusivity sources will be quantified through the following magnitudes, the non-dimensional values of the viscosity-like quantity proposed by Park and Moin, ν_{ap}/ν, for the apparent diffusive effects, and $\nu_{T,wm}/\nu$ for the modeled diffusivity.

DOI: 10.13009/EUCASS2019-694

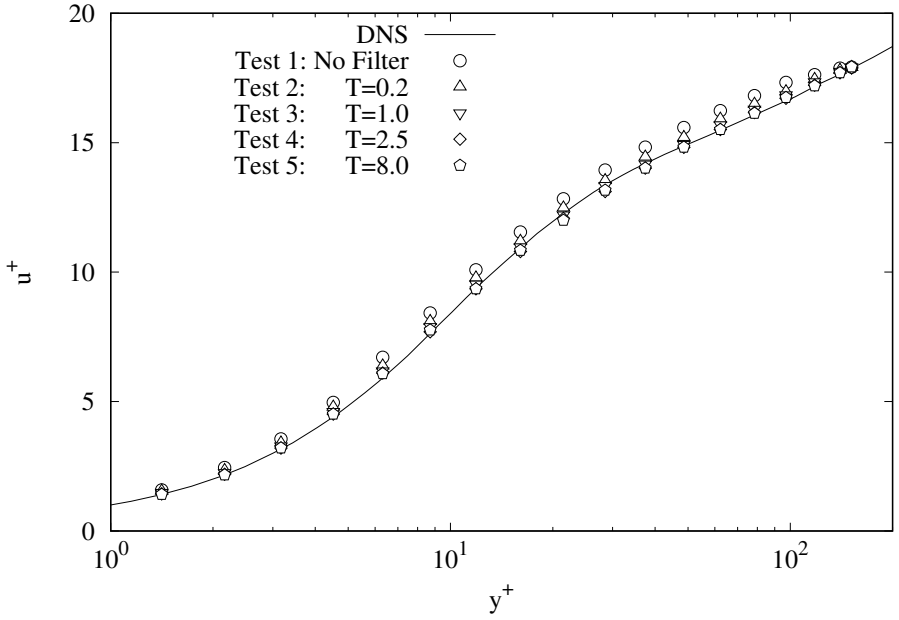

Figure 4: Mean streamwise velocity profile of a pipe flow at $Re_\tau \approx 500$. Comparison between DNS data and the WM mean velocity field for five different configurations.

The application of the TAF almost completely suppresses the apparent diffusive effects of the RRS in the wall domain, even with the smallest filter length (see Figure 5 on the left). This is consistent with the fact that the smallest filtering period, $T_1 = 0.2$, suppresses the LES dissipation range frequencies. However, according to the wall shear stress results, the fact of completely suppressing the apparent diffusive component does not yield satisfactory results. We find the explanation in the RANS model behavior, which provides the modeled diffusive component. Good results are not obtained until suppressing frequencies higher than the energy-containing/inertial range limit. By inspecting Figure 5 on the right, we observe that for smaller filter lengths, particularly $T_1 = 0.2$, although the apparent component is eliminated, the modeled component is still overpredicted. This is coherent with the fact that RANS models only expect mean-flow-based quantities both, within their inner computational domains and at their boundaries. When introducing time-resolved data in a RANS domain, despite its characteristic frequencies do not have apparent diffusive effects, they make the RANS model working out of range. According to the results, only very large scale fluctuations in the energy-containing range are compatible with the RANS physical model.

According to the mixing-length-based RANS model (see Equation 5), the excessive levels of ν_{Twm} are due to an overpredicted value of the rate-of-strain tensor magnitude, $|S|$, which is caused by the additional components of $S(U)$ steaming from the LES time-resolved data. On the other hand, the Van Driest wall-damping function could not cause the unphysical ν_{Twm} values, since erroneous values of y^+ derived from a wall shear stress overprediction, would shrink the function damping region towards the wall.

In summary, blocking the LES highest frequencies and their apparent dissipative effects is essential to have an appropriate diffusivity level within the RANS domain. All the techniques published so far intended to neutralize the RRS effects, only place the focus on this source of inappropriate diffusivity for a RANS context.[5,11,15] Nonetheless, it is not sufficient since time-resolved data also affects the modeled diffusivity levels. According to Larsson *et al.*, for a RANS model, the model quantities should be exclusively derived from the mean velocity field, or very-large-scale unsteady motions at most.[12] According to the results, the inertial subrange motions have an unphysical contribution to the rate-of-strain magnitude which leads to an incorrect evaluation of ν_T, whereas only the lowest frequencies of the energy-containing range do not significantly affect the RANS model output. As a conclusion, the minimum filter cut-off length has to be set at the energy-containing/inertial range limit , which in the present test corresponds to $T_3 = 1$. It is worth to comment that, in this particular case of a steady equilibrium flow, by increasing the filtering period well into the energy-containing range, the results remain almost unaffected as observed with tests T_4 and T_5.

DOI: 10.13009/EUCASS2019-694

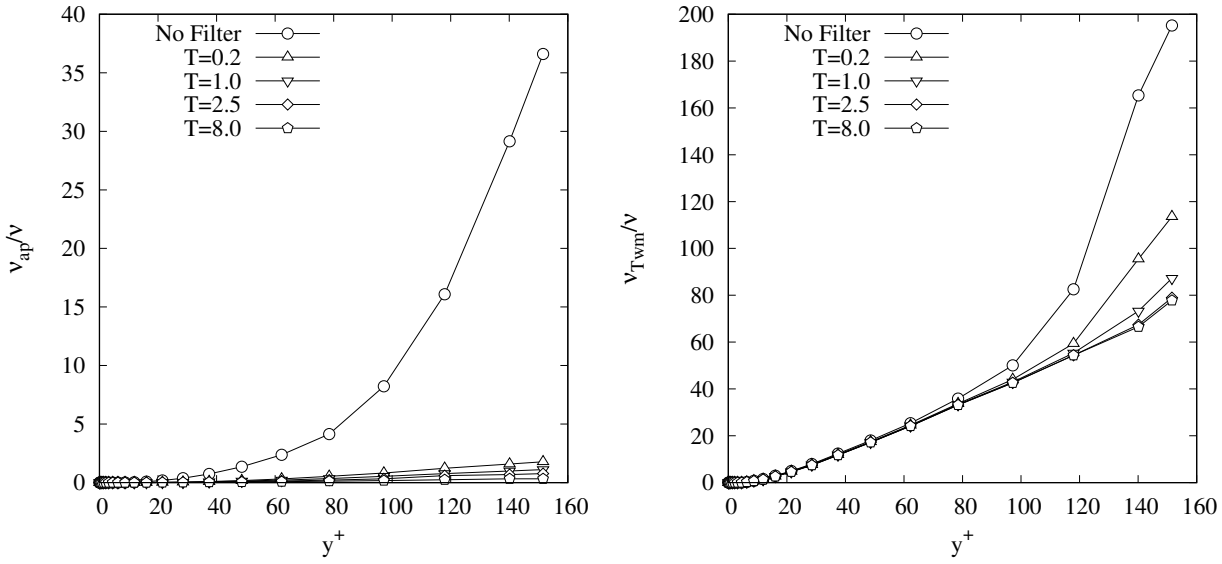

Figure 5: Left: Normalized viscosity obtained with the Park and Moin methodology as a measure of the RRS apparent diffusive effects ($\nu_{ap}/\nu = -R(\mathbf{U})S(\mathbf{U})/2\nu S(\mathbf{U})S(\mathbf{U})$). Right: Normalized turbulent viscosity (ν_{Twm}/ν). Both magnitudes are plotted vs. the wall distance in wall units and within the wall layer.

Wall model validation test: Pipe flow at $Re_\tau \approx 3000$

The present test is intended to validate the methodologies proposed in the previous Section in regular operation conditions, i.e., with the wall model feeding back the LES computation with the wall shear stress output. The proposed case is an equilibrium pipe flow at $Re_\tau \approx 3000$. The validation will be carried out with three different configurations, an LES-only test with no specific wall treatment, a non-filtered WMLES, and a filtered WMLES with several different filtering widths. The computational setup for the LES domain is the same as in the previous Section but with WMLES grid spacing requirements.[9] Specifically, $\Delta z^+ = 236$, $\Delta r\theta^+ = 198$ at $r = R$ and $\Delta r^+ = 60$, being the first off-wall LES nodes placed at $y_1^+ = 30$, which is the WM/LES interface position. The WM mesh resolution in the wall-normal direction is 10 point with the nodes concentrated towards the wall, being the position of the first off-wall nodes $y^+ \approx 0.1$. The grid spacings in the other directions are common with the LES mesh. Regarding the subgrid strategy, the dynamic Smagorinsky model of Germano,[10] as in previous cases, is used.

In order to determine the different filter lengths to be tested, the methodology presented in the previous Section has been used. A numerical probe has been placed at the WM/LES interface at $y^+ = 30$, and the temporal signal of the main problem variables has been obtained for approximately ten flow-through periods, i.e., $100\,TU$, in order to ensure that all flow motions present in that region, are captured in the energy spectrum. In Figure 6, the power spectrum of the most characteristic variable, the streamwise velocity component, is shown. Several time-filtering periods have been selected along the power spectrum curve according to the criteria established in the previous section. These values are summarized in Table 3 together with their position within the power spectrum.

Table 3: Summary of the different WMLES configurations tested with the $Re_\tau \approx 3000$ Pipe Flow.

Test number (n)	$f_n = 1/T_n$	Filter length T_n	Energy spectrum range
1	no wall model	N/A	N/A
2	no filter	N/A	N/A
3	1.8	0.55	inertial/dissipation range limit
4	0.5	2.0	inertial/energy-containing range limit
5	0.25	4.0	within the energy-containing range
6	0.1	10.0	flow-through period, largest flow scales

DOI: 10.13009/EUCASS2019-694

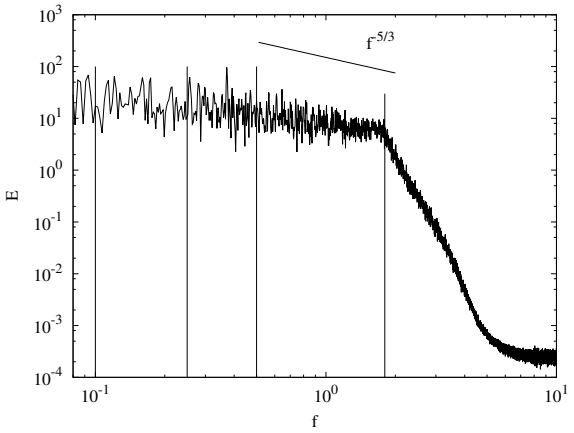

Figure 6: Power spectrum of the streamwise velocity component at $y^+ \approx 30$ of a Pipe flow at $Re_\tau \approx 3000$.

Pipe flow at $Re_\tau \approx 3000$ test results

In table 4, the computed Re_τ value as a measure of the wall shear stress is displayed. The conclusions obtained in previous sections are confirmed in the present test with the wall model operating in regular conditions. As the filter length increases, the error in the wall shear stress evaluation gets reduced until it remains constant regardless of the filter size. The point in which the filter-length independence is reached starts approximately in the energy-containing/inertial subrange limit, which is coherent with the observation in the filter efficiency test presented above. On the other hand, good results are obtained by applying very large time-averaging periods ($T_6 = 10$), suggesting that in equilibrium steady-state conditions, providing accurate time-averaged shear stress to the LES boundary, is sufficient to keep an appropriate global momentum balance.

Table 4: TAF efficiency test results performed with a channel flow at $Re_\tau \approx 3000$. The computed Re_τ and its relative error with respect to the target value ($Re_\tau \approx 3026$) is shown.

Test (n)	Filter length T_n	Computed Re_τ	rel. err. [%]
1	no wall model	1923.6	36.40
2	no filter	3409.2	12.66
3	0.55	3201.18	5.78
4	2.0	3141.34	3.81
5	4.0	3138.09	3.70
6	10.0	3135.6	3.62

The mean velocity profiles subsequently confirm the wall shear stress results. In Figure 7, the time-averaged streamwise velocity component is displayed for four different configurations. The tests featuring the largest filter-lengths, i.e. $T_5 = 4$ and $T_6 = 10$, they have not been included for the sake of clarity since no differences were observed with respect to the $T_3 = 2$ configuration. Again, good agreement with DNS data of Ahn *et al.*[1] is obtained when filtering frequencies from the energy-containing/inertial subrange limit upwards.

Conclusions

The application of a time-average filter is proposed for the first time in the Two-Layer wall model context in order to prevent the LES time-resolved data from entering the wall model RANS-based domain. The efficiency of the methodology is assessed with a numerical experiment based on a $Re_\tau \approx 500$ pipe flow, and further validated with a high Reynolds number pipe flow at $Re_\tau \approx 3000$ in regular WMLES operating conditions.

The main purpose of the temporal filter in the TLM context is avoiding the unwanted effects of the resolved Reynolds stresses when entering the wall model domain. To the author's best knowledge, all methodologies proposed so far with the purpose of suppressing the RRS detrimental effects,[5,11,15] placed the focus on the RRS apparent-

DOI: 10.13009/EUCASS2019-694

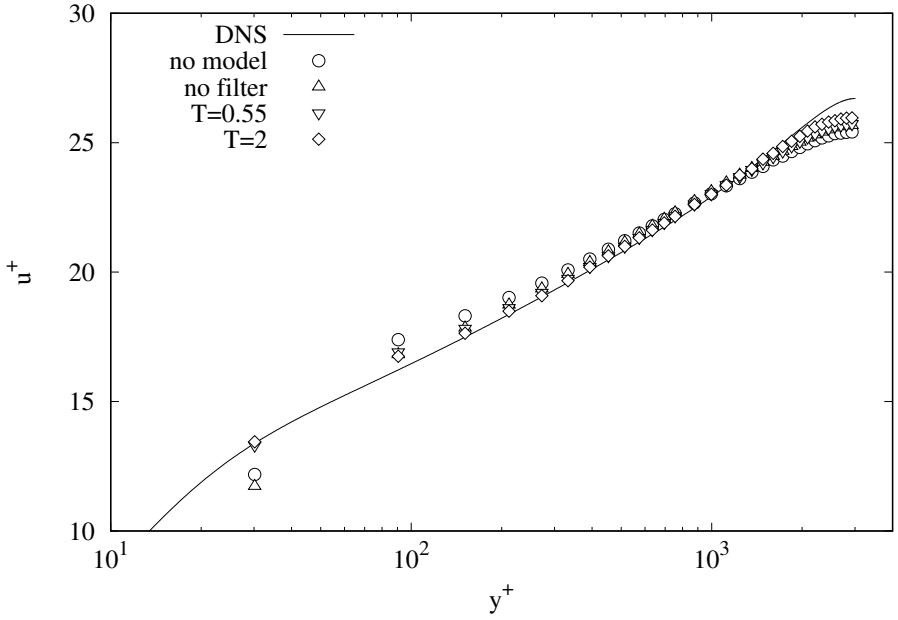

Figure 7: Mean streamwise velocity profile of a pipe flow at $Re_\tau \approx 3000$. Comparison between DNS data[1] and the WM mean velocity field for four different configurations.

diffusive effects on the wall model domain. Nevertheless, according to the results obtained in the present work, the apparent diffusive effects are only part of the problem. RANS models are intended to simulate only the mean flow component. Thus, no turbulent flow structures are resolved and their effects on the mean flow are fully modeled and taken into account through the turbulent viscosity, ν_T, provided by the RANS model. Therefore, since no temporal data is resolved, ν_T must be derived with the only available data corresponding to the mean velocity field. When forcing the inflow of time-resolved data through the boundary, the regular working conditions of the RANS-based domain are disrupted. This disruption is not only caused by the apparent diffusivity of the resolved turbulent structures, but it is also caused because the fluctuating velocity field makes the RANS model to work out of its range of applicability since it is fed with inadequate input data. The temporal filter applied to the WM/LES interface suppresses with a simple and low-computational cost step this recurrent problem. On the other hand, a methodology based on the velocity power spectrum is proposed to determine the optimal filter length required to avoid the RRS spurious effects. It is concluded that the energy-containing/inertial subrange limit is an adequate filter width which suppresses the harmful frequencies while taking into account the largest flow scales. Finally, according to the results, the other characteristic problem affecting the TLM approach, the "log layer mismatch" is also greatly mitigated by the temporal filter. This is in line with the findings of Yang *et al.* who first pointed out this effect in a previous work[21] but in the context of a simple equilibrium wall function based on the log-law.

Acknowledgements

This work has been financially supported by the Ministerio de Economía y Competitividad, Spain (ENE2017-88697-R) and by a Ramón y Cajal postdoctoral contract (RYC-2012-11996). The authors thankfully acknowledge the institutions. Special thanks to Junsun Ahn and Hyung Jin Sung for providing results that allowed comparison in the pipe flow at $Re_\tau \approx 3000$ test.

References

[1] J. Ahn, J. H. Lee, J. Lee, J. H. Kang, and H. J. Sung. Direct numerical simulation of a 30R long turbulent pipe flow at $\mathrm{Re}_\tau = 3008$. *Phys. Fluids*, 27:065110, 2015.

DOI: 10.13009/EUCASS2019-694

[2] E. Balaras and C. Benocci. Subgrid-scale models in finite-difference simulations of complex wall bounded flows. In *AGARD CP 551*, pages 2.1–2.5, 1994.

[3] E. Balaras, C. Benocci, and U. Piomelli. Two-layer approximate boundary conditions for large-eddy simulations. *AIAA J.*, 34 (6):1111–1119, 1996.

[4] W. Cabot. Near-wall models in large-eddy simulations of flow behind a backward-facing step. *Annual Research Brief. Center for Turbulence Research, Stanford, CA*, pages 199–210, 1996.

[5] W. Cabot and P. Moin. Approximate wall boundary conditions in the large-eddy simulation of high Reynolds number flow. *Flow Turbul. Combust.*, 63:269–291, 1999.

[6] J. Calafell, F.X. Trias, O. Lehmkuhl, and A. Oliva. A time-average filtering technique to imporve the efficiency of two-layer wall models for large eddy simulation in complex geometries. *Comput. Fluids*, 188:44–59, 2019.

[7] A. Carmona, O. Lehmkuhl, C. D. Pérez-Segarra, and A. Oliva. Numerical analysis of the transpose diffusive term for viscoplastic-type non-newtonian fluid flows using a collocated variable arrangement. *Numer. Heat Tr. B-Fund.*, 67:410–436, 2015.

[8] C. Chin, A. S. H. Ooi, I. Marusic, and H. M. Blackburn. The influence of pipe length on turbulence statistics computed from direct numerical simulation data. *Phys. Fluids*, 22:115107, 2010.

[9] H. Choi and P. Moin. Grid-point requirements for large eddy simulation: Chapman's estimates revisited. *Phys. Fluids*, 24:011702, 2012.

[10] M. Germano, U. Piomelli, P. Moin, and W. Cabot. A dynamic subgrid-scale eddy viscosity model. *Phys. Fluids*, 3:1760–1765, 1991.

[11] S. Kawai and J. Larsson. Wall-modeling in large eddy simulation: Length scales, grid resolution, and accuracy. *Phys. Fluids*, 24:015105, 2012.

[12] S. Lardeau and M. Leschziner. Unsteady Reynolds-Averaged Navier-Stokes computations of transitional wake/blade interaction. *AIAA J.*, 42(8):1559–1571, 2004.

[13] J. Larsson, S. Kawai, J. Bodart, and I. Bermejo-Moreno. Large-eddy simulation with modeled wall-stress: recent progress and future directions. *Mech. Engng. Rev.*, 3(1):1–23, 2016.

[14] D. K. Lilly. A proposed modification of the Germano subgrid-scale closure method. *Phys. Fluids*, 4:633–635, 1992.

[15] G. I. Park and P. Moin. An improved dynamic non-equilibrium wall-model for large eddy simulation. *Phys. Fluids*, 26:015108, 2014.

[16] G. I. Park and P. Moin. Numerical aspects and implementation of a two-layer zonal wall model for LES of compressible turbulent flows on unstructured meshes. *J. Comput. Phys.*, 305:589–603, 2016.

[17] U. Piomelli and E. Balaras. Wall-layer models for large-eddy simulations. *Annu. Rev. Fluid Mech.*, 34:349–374, 2002.

[18] S. B. Pope. *Turbulent flows.* Cambridge Univesity Press, 2000.

[19] F. X. Trias and O. Lehmkuhl. A self-adaptive strategy for the time-integration of Navier-Stokes equations. *Numer. Heat Tr. B-Fund.*, 60-2:116–134, 2011.

[20] R. W. C. P. Verstappen and A. E. P. Veldman. Symmetry-preserving discretization of turbulent flow. *J. Comput. Phys.*, 187:343–368, 2003.

[21] X. I. A. Yang, G. I. Park, and P. Moin. Log-layer mismatch and modeling of the fluctuating wall stress in wall-modeled large-eddy simulations. *Phys. Rev. Fluids*, 2:104601, 2017.

[22] X. I. A. Yang, J. Sadique, R. Mittal, and C. Meneveau. Integral wall model for large eddy simulations of wall-bounded turbulent flows. *Phys. Fluids*, 27:025112, 2015.